

# A Study of $D^0 \rightarrow K_S^0 K_S^0 X$ Decay Channels

The FOCUS Collaboration<sup>\*</sup>

J. M. Link<sup>a</sup>, P. M. Yager<sup>a</sup>, J. C. Anjos<sup>b</sup>, I. Bediaga<sup>b</sup>,  
 C. Göbel<sup>b</sup>, A. A. Machado<sup>b</sup>, J. Magnin<sup>b</sup>, A. Massafferri<sup>b</sup>,  
 J. M. de Miranda<sup>b</sup>, I. M. Pepe<sup>b</sup>, E. Polycarpo<sup>b</sup>,  
 A. C. dos Reis<sup>b</sup>, S. Carrillo<sup>c</sup>, E. Casimiro<sup>c</sup>, E. Cuautle<sup>c</sup>,  
 A. Sánchez-Hernández<sup>c</sup>, C. Uribe<sup>c</sup>, F. Vázquez<sup>c</sup>, L. Agostino<sup>d</sup>,  
 L. Cinquini<sup>d</sup>, J. P. Cumalat<sup>d</sup>, B. O'Reilly<sup>d</sup>, I. Segoni<sup>d</sup>,  
 K. Stenson<sup>d</sup>, J. N. Butler<sup>e</sup>, H. W. K. Cheung<sup>e</sup>, G. Chiodini<sup>e</sup>,  
 I. Gaines<sup>e</sup>, P. H. Garbincius<sup>e</sup>, L. A. Garren<sup>e</sup>, E. Gottschalk<sup>e</sup>,  
 P. H. Kasper<sup>e</sup>, A. E. Kreymer<sup>e</sup>, R. Kutschke<sup>e</sup>, M. Wang<sup>e</sup>,  
 L. Benussi<sup>f</sup>, M. Bertani<sup>f</sup>, S. Bianco<sup>f</sup>, F. L. Fabbri<sup>f</sup>, A. Zallo<sup>f</sup>,  
 M. Reyes<sup>g</sup>, C. Cawfield<sup>h</sup>, D. Y. Kim<sup>h</sup>, A. Rahimi<sup>h</sup>, J. Wiss<sup>h</sup>,  
 R. Gardner<sup>i</sup>, A. Kryemadhi<sup>i</sup>, Y. S. Chung<sup>j</sup>, J. S. Kang<sup>j</sup>,  
 B. R. Ko<sup>j</sup>, J. W. Kwak<sup>j</sup>, K. B. Lee<sup>j</sup>, K. Cho<sup>k</sup>, H. Park<sup>k</sup>,  
 G. Alimonti<sup>l</sup>, S. Barberis<sup>l</sup>, M. Boschini<sup>l</sup>, A. Cerutti<sup>l</sup>,  
 P. D'Angelo<sup>l</sup>, M. DiCorato<sup>l</sup>, P. Dini<sup>l</sup>, L. Edera<sup>l</sup>, S. Erba<sup>l</sup>,  
 P. Inzani<sup>l</sup>, F. Leveraro<sup>l</sup>, S. Malvezzi<sup>l</sup>, D. Menasce<sup>l</sup>,  
 M. Mezzadri<sup>l</sup>, L. Moroni<sup>l</sup>, D. Pedrini<sup>l</sup>, C. Pontoglio<sup>l</sup>,  
 F. Prelz<sup>l</sup>, M. Rovere<sup>l</sup>, S. Sala<sup>l</sup>, T. F. Davenport III<sup>m</sup>,  
 V. Arena<sup>n</sup>, G. Boca<sup>n</sup>, G. Bonomi<sup>n</sup>, G. Gianini<sup>n</sup>, G. Liguori<sup>n</sup>,  
 D. Lopes Pegna<sup>n</sup>, M. M. Merlo<sup>n</sup>, D. Pantea<sup>n</sup>, S. P. Ratti<sup>n</sup>,  
 C. Riccardi<sup>n</sup>, P. Vitulo<sup>n</sup>, H. Hernandez<sup>o</sup>, A. M. Lopez<sup>o</sup>,  
 H. Mendez<sup>o</sup>, A. Paris<sup>o</sup>, J. Quinones<sup>o</sup>, J. E. Ramirez<sup>o</sup>,  
 Y. Zhang<sup>o</sup>, J. R. Wilson<sup>p</sup>, T. Handler<sup>q</sup>, R. Mitchell<sup>q</sup>,  
 D. Engh<sup>r</sup>, M. Hosack<sup>r</sup>, W. E. Johns<sup>r</sup>, E. Luiggi<sup>r</sup>, J. E. Moore<sup>r</sup>,  
 M. Nehring<sup>r</sup>, P. D. Sheldon<sup>r</sup>, E. W. Vaandering<sup>r</sup>, M. Webster<sup>r</sup>,  
 M. Sheaff<sup>s</sup>

<sup>a</sup>University of California, Davis, CA 95616

<sup>b</sup>Centro Brasileiro de Pesquisas Físicas, Rio de Janeiro, RJ, Brasil

<sup>c</sup>CINVESTAV, 07000 México City, DF, Mexico

<sup>\*</sup> See <http://www-focus.fnal.gov/authors.html> for additional author information.

- <sup>d</sup>*University of Colorado, Boulder, CO 80309*  
<sup>e</sup>*Fermi National Accelerator Laboratory, Batavia, IL 60510*  
<sup>f</sup>*Laboratori Nazionali di Frascati dell'INFN, Frascati, Italy I-00044*  
<sup>g</sup>*University of Guanajuato, 37150 Leon, Guanajuato, Mexico*  
<sup>h</sup>*University of Illinois, Urbana-Champaign, IL 61801*  
<sup>i</sup>*Indiana University, Bloomington, IN 47405*  
<sup>j</sup>*Korea University, Seoul, Korea 136-701*  
<sup>k</sup>*Kyungpook National University, Taegu, Korea 702-701*  
<sup>l</sup>*INFN and University of Milano, Milano, Italy*  
<sup>m</sup>*University of North Carolina, Asheville, NC 28804*  
<sup>n</sup>*Dipartimento di Fisica Nucleare e Teorica and INFN, Pavia, Italy*  
<sup>o</sup>*University of Puerto Rico, Mayaguez, PR 00681*  
<sup>p</sup>*University of South Carolina, Columbia, SC 29208*  
<sup>q</sup>*University of Tennessee, Knoxville, TN 37996*  
<sup>r</sup>*Vanderbilt University, Nashville, TN 37235*  
<sup>s</sup>*University of Wisconsin, Madison, WI 53706*

---

## Abstract

Using data from the FOCUS experiment (FNAL-E831), we report on the decay of  $D^0$  mesons into final states containing more than one  $K_S^0$ . We present evidence for two Cabibbo favored decay modes,  $D^0 \rightarrow K_S^0 K_S^0 K^- \pi^+$  and  $D^0 \rightarrow K_S^0 K_S^0 K^+ \pi^-$ , and measure their combined branching fraction relative to  $D^0 \rightarrow \bar{K}^0 \pi^+ \pi^-$  to be  $\frac{\Gamma(D^0 \rightarrow K_S^0 K_S^0 K^\pm \pi^\mp)}{\Gamma(D^0 \rightarrow \bar{K}^0 \pi^+ \pi^-)} = 0.0106 \pm 0.0019 \pm 0.0010$ . Further, we report new measurements of  $\frac{\Gamma(D^0 \rightarrow K_S^0 K_S^0 K_S^0)}{\Gamma(D^0 \rightarrow \bar{K}^0 \pi^+ \pi^-)} = 0.0179 \pm 0.0027 \pm 0.0026$ ,  $\frac{\Gamma(D^0 \rightarrow K^0 \bar{K}^0)}{\Gamma(D^0 \rightarrow \bar{K}^0 \pi^+ \pi^-)} = 0.0144 \pm 0.0032 \pm 0.0016$ , and  $\frac{\Gamma(D^0 \rightarrow K_S^0 K_S^0 \pi^+ \pi^-)}{\Gamma(D^0 \rightarrow \bar{K}^0 \pi^+ \pi^-)} = 0.0208 \pm 0.0035 \pm 0.0021$  where the first error is statistical and the second is systematic.

---

## 1 Introduction

Detailed measurements of rare exclusive decay modes of charm mesons provide a powerful way to probe the details of charm decay such as the contributions of  $W$  exchange diagrams and final state interactions. These measurements aid our understanding of the interplay between the weak and strong interactions, mainly for multibody decays where theoretical predictions are poorer than for two body decays. We report the first observation of  $D^0 \rightarrow K_S^0 K_S^0 \pi^\pm K^\mp$ , and new measurements of  $D^0 \rightarrow K_S^0 K_S^0 K_S^0$ ,  $D^0 \rightarrow K_S^0 K_S^0$ , and  $D^0 \rightarrow K_S^0 K_S^0 \pi^+ \pi^-$ .

The fixed-target charm photoproduction experiment FOCUS, an upgraded version of E687 [1], collected data during the 1996–1997 fixed-target run at Fermilab. A photon beam is derived from the bremsstrahlung of secondary electrons and positrons produced from the 800 GeV/ $c$  Tevatron proton beam. The photon beam interacts with a segmented beryllium-oxide target. The average photon energy for reconstructed charm events is 180 GeV.

Two silicon microvertex systems provide excellent separation between the production and charm decay vertices. One silicon strip detector called target silicon (TS) is embedded in the BeO target segments [2]. The other silicon strip detector (SSD) is located downstream of the target region. Charged particles are tracked and momentum analyzed with five stations of multiwire proportional chambers in a two magnet forward spectrometer. Three multi-cell threshold Čerenkov detectors are implemented to identify electrons, pions, kaons, and protons [3].

## 2 Reconstruction of individual particles: $K_S^0$ , $K$ , and $\pi$

A detailed description of individual  $K_S^0$  reconstruction in the FOCUS spectrometer can be found elsewhere [4]. Briefly,  $K_S^0$ 's are identified in several different regions depending on the  $K_S^0$  decay length; upstream of the magnet with silicon strip information, upstream of the magnet without silicon strip information, and inside of the magnet. Depending on whether the daughter pions from the  $K_S^0$  pass through the second magnet, and hence have a well defined momentum, a series of different techniques are employed. Roughly 15% of the  $K_S^0$  are found upstream of the silicon system and can be used in locating the  $D^0$  decay vertex. When there are two or more  $K_S^0$  in a decay channel, the daughter tracks must all be distinct and can not be shared between  $K_S^0$  candidates. The reconstructed mass of the  $K_S^0$  must be within three standard deviations of the nominal  $K_S^0$  mass.

All charged tracks from the charm decay must be singly linked to the silicon microstrip, be of good quality, and inconsistent with zero degree photon conversion. Čerenkov particle identification (PID) for charged particles is performed by constructing a log likelihood value  $\mathcal{W}_i$  for the particle hypotheses ( $i = e, \pi, K, p$ ). The  $\pi$  consistency of a track is defined by  $\Delta\mathcal{W}_\pi = \mathcal{W}_{min} - \mathcal{W}_\pi$ , where  $\mathcal{W}_{min}$  is the minimum  $\mathcal{W}$  value of the other three hypotheses. Similarly, we define  $\Delta\mathcal{W}_{K,\pi} = \mathcal{W}_\pi - \mathcal{W}_K$  and  $\Delta\mathcal{W}_{K,p} = \mathcal{W}_p - \mathcal{W}_K$  for kaon identification and we require  $\Delta\mathcal{W}_{K,\pi} > 1$  and  $\Delta\mathcal{W}_{K,p} > -2$  for kaons and  $\Delta\mathcal{W}_\pi > -5$  for pions.

### 3 Reconstruction of $D^0$ candidates

The  $D^0$  candidates are formed by making a vertex hypothesis for the daughter particles whenever possible. We use the  $K_S^0$  candidates and two charged tracks of the correct charge combination to form a  $D^0$  candidate. The confidence level of the decay vertex of the  $D^0$  candidate is required to be greater than 1%. The combined momentum vector located at the decay vertex forms the  $D^0$  track. Using the  $D^0$  track as a seed track for the candidate driven vertexing algorithm [1], we search for a production vertex in which the confidence level is greater than 1% and the primary multiplicity including the seed track must have at least 3 tracks. The production vertex must be inside the target. The significance of separation between the production and the decay vertices ( $L/\sigma_L$ ) must be greater than 4 for  $D^0 \rightarrow K_S^0 K_S^0 \pi^\mp K^\pm$  and greater than 6 for  $D^0 \rightarrow K_S^0 K_S^0 \pi^+ \pi^-$ . Different values are chosen for the  $L/\sigma_L$  cut due to the level of background for the two channels, but scans are performed in  $L/\sigma_L$  as part of the systematic uncertainty studies.

A stand-alone vertex algorithm is used to reconstruct the primary vertex of the event for decay modes without charged tracks [1]. All the silicon microvertex tracks in the event, excluding those already assigned to pions used to reconstruct  $K_S^0$ , are used to form all possible vertices of the event with a confidence level greater than 1%: we then choose the primary vertex to be the highest multiplicity vertex. Ties are resolved choosing the most upstream vertex.

The signal channels are normalized to  $D^0 \rightarrow \bar{K}^0 \pi^+ \pi^-$  which is the most abundant  $D^0$  decay mode containing a  $K_S^0$ . We use only the most basic cuts in this analysis. The invariant mass distribution for  $D^0 \rightarrow K_S^0 \pi^+ \pi^-$  at an  $L/\sigma_L > 4$  is presented in Fig. 1a. To determine the reconstruction efficiency of this channel we use a Monte Carlo simulation using our best determined decay distribution to generate  $D^0 \rightarrow \bar{K}^0 \pi^+ \pi^-$ . The reconstructed Monte Carlo sample was six times larger than the data sample. We fit our signals from both data and Monte Carlo with a Gaussian for the signal and a  $2^{nd}$  degree polynomial for the background using a maximum likelihood fit. As our most copious  $K_S^0$  decay channel, we use the  $D^0 \rightarrow K_S^0 \pi^+ \pi^-$  mode to search for variations versus reconstructed  $K_S^0$  categories. We identify a systematic uncertainty on  $K_S^0$  reconstruction of 7.1%.

The systematic uncertainty for each branching fraction is independently determined. Several tests are performed. To check the stability of the branching fractions we fix the cuts to their standard values and vary one cut at a time. Cuts which are scanned include particle identification, significance of separation, isolation of the secondary vertex from any other track, and confidence level of the secondary vertex. We also perform split sample systematics by dividing our samples into two sub-samples based on momentum and data-

taking period. We study fit variant systematics by calculating the branching fraction when the signals are fit with 1<sup>st</sup>, 2<sup>nd</sup>, or 3<sup>rd</sup> degree polynomials.

We look for Monte Carlo resonance systematics by searching for a difference in reconstruction efficiency between non-resonant generation and a specific resonance channel. We also include a systematic uncertainty for the absolute tracking efficiency (0.2% per difference in numbers of tracks) and for  $K_S^0$  reconstruction efficiency (7.1% per  $K_S^0$ ). Finally, we include a small contribution to the systematic uncertainty due to Monte Carlo statistics. All systematic uncertainties are added in quadrature.

#### 4 The $D^0 \rightarrow K_S^0 K_S^0 K^\pm \pi^\mp$ Decay Mode

The  $D^0$  final state  $K_S^0 K_S^0 K^\pm \pi^\mp$  has not been observed by previous experiments. While the  $D^0$  decay modes  $D^0 \rightarrow \bar{K}^0 \bar{K}^0 K^+ \pi^-$ ,  $D^0 \rightarrow \bar{K}^0 K^0 K^- \pi^+$ , and  $D^0 \rightarrow \bar{K}^0 K^0 K^+ \pi^-$  can result in a final state  $K_S^0 K_S^0 K^\pm \pi^\mp$ , the decay mode  $D^0 \rightarrow \bar{K}^0 K^0 K^+ \pi^-$  is doubly Cabibbo suppressed and we assume that this mode is small compared to the other two Cabibbo favored modes. To distinguish the two Cabibbo favored decays we use the charge of the soft pion in the decay sequence  $D^{*+} \rightarrow D^0 \pi^+$ . First, we demonstrate a signal for the two channels combined without using a soft pion tag and then we argue that we have evidence for independent observations in both channels. In Fig. 1b we show the invariant mass plot for  $D^0 \rightarrow K_S^0 K_S^0 K^\pm \pi^\mp$  at  $L/\sigma > 4$ . We fit the plot with a Gaussian for the signal and a 2<sup>nd</sup> degree polynomial for the background using a maximum likelihood fit and we find  $57 \pm 10$  events.

We find no evidence for resonant substructure in  $D^0 \rightarrow K_S^0 K_S^0 K^\pm \pi^\mp$  and use a non-resonant Monte Carlo simulation to obtain the efficiency. As a systematic check we find a 2.6% difference in efficiency from a  $D^0 \rightarrow a_0(980)^+ K^*(892)^-$  Monte Carlo simulation.

Correcting for efficiency, we find:

$$\frac{\Gamma(D^0 \rightarrow K_S^0 K_S^0 K^\pm \pi^\mp)}{\Gamma(D^0 \rightarrow \bar{K}^0 \pi^+ \pi^-)} = 0.0106 \pm 0.0019 \pm 0.0010. \quad (1)$$

We have included systematic uncertainty contributions from split samples (0), fit variations (0.0007), possible resonant decay (0.0001), Monte Carlo statistics (0.0001), absolute tracking efficiency (0.0001), and variation between  $K_S^0$  reconstruction categories (0.00075).

While we have established that we see a new decay channel, in order to separate  $D^0 \rightarrow K_S^0 K_S^0 K^+ \pi^-$  and  $D^0 \rightarrow K_S^0 K_S^0 K^- \pi^+$  we need to tag a  $D^0$  by using

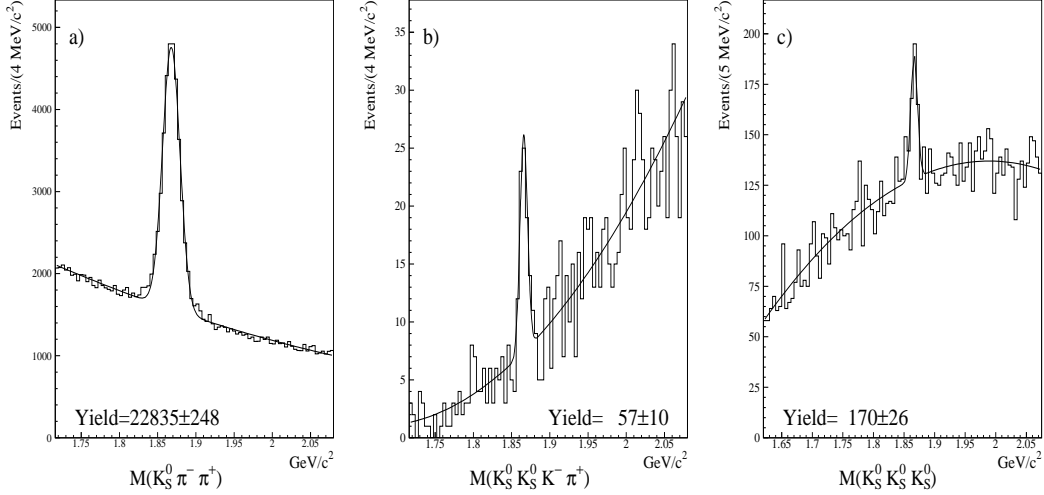


Fig. 1. Invariant mass distribution for various  $D^0$  final states: (a) Reconstructed mass of  $D^0 \rightarrow K_S^0 \pi^+ \pi^-$ . There are  $22835 \pm 248$  events with a sigma of  $11.4 \text{ MeV}/c^2$ . (b) Reconstructed mass of  $D^0 \rightarrow K_S^0 K_S^0 K^\pm \pi^\mp$ . There are  $57 \pm 10$  events with a sigma of  $5.0 \text{ MeV}/c^2$ . (c) Reconstructed mass of  $D^0 \rightarrow K_S^0 K_S^0 K_S^0$ . There are  $170 \pm 26$  events with a sigma of  $5.6 \text{ MeV}/c^2$ .

the soft pion from the  $D^{*+} \rightarrow D^0 \pi^+$  decay. In Fig. 2c we present the mass difference  $M(K_S^0 K_S^0 K^\pm \pi^\mp \pi_s) - M(K_S^0 K_S^0 K^\pm \pi^\mp)$  in which we find  $14.1 \pm 4.4$  signal events when we cut around the  $D^0$  mass. Fig. 2a (2b) shows the mass difference histogram for the events in which the soft pion has the opposite (same) charge as that of the kaon. The two histograms show a signal of  $7.2 \pm 3.4$  and  $6.8 \pm 2.9$  events, respectively. The fits in all three histograms are performed by fixing the mass and width to the values returned from the Monte Carlo.

## 5 The $D^0 \rightarrow K_S^0 K_S^0 K_S^0$ Decay Mode

Although this mode is Cabibbo allowed, it requires either final state interactions or  $W$ -exchange to occur. Due to the limited phase space and the need to identify three  $K_S^0$  candidates, the signal can be observed without the need for a  $D^{*+}$  tag or a  $L/\sigma_L$  cut. This significantly improves the reconstruction efficiency. In Fig. 1c we find a signal of  $170 \pm 26$  events.

We find no evidence for resonant substructure and use a non-resonant Monte Carlo simulation to obtain the efficiency. A  $D^0 \rightarrow a_0(980)^0 K_S^0$  simulation is used as a measure of the systematic variation (the difference in efficiency is 5.6 %). For the branching ratio of this mode with respect to the  $D^0 \rightarrow \bar{K}^0 \pi^+ \pi^-$  mode we find:

$$\frac{\Gamma(D^0 \rightarrow K_S^0 K_S^0 K_S^0)}{\Gamma(D^0 \rightarrow \bar{K}^0 \pi^+ \pi^-)} = 0.0179 \pm 0.0027 \pm 0.0026. \quad (2)$$

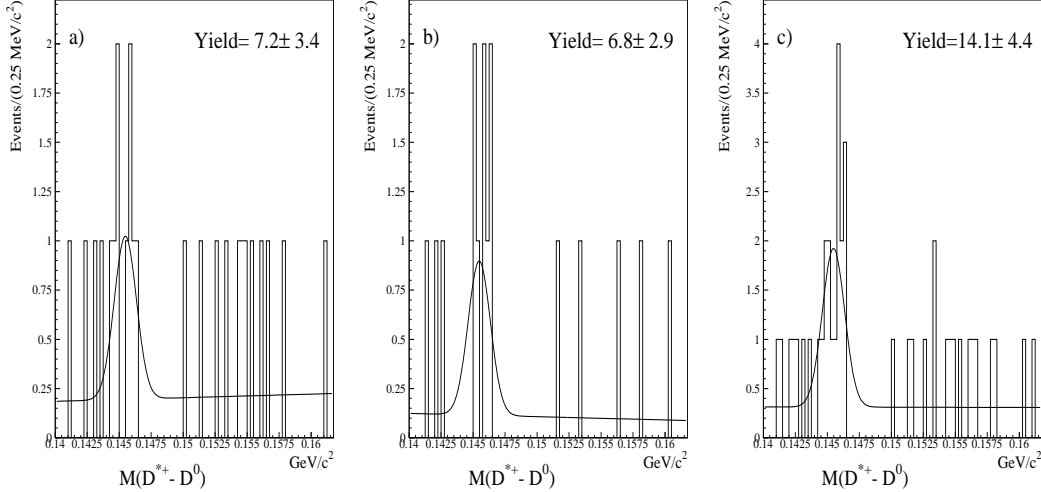


Fig. 2. Mass difference between  $M(K_S^0 K_S^0 K^\pm \pi^\mp \pi_s)$  and  $M(K_S^0 K_S^0 K^\pm \pi^\mp)$  where  $\pi_s$  is a pion from the primary vertex. Plots a, b, and c are for cases where the  $\pi_s$  charge relative to the kaon charge is opposite, same, or either, respectively. A mass cut of  $1.85 < M(K_S^0 K_S^0 K^\pm \pi^\mp \pi_s) < 1.88 \text{ GeV}/c^2$  to select  $D^0$  events is applied.

We have included systematic uncertainty contributions from split samples (0), fit variations (0.0007), possible resonant decay (0.0005), Monte Carlo statistics (0.0001), absolute tracking efficiency (0.0001), and the variation between  $K_S^0$  reconstruction categories (0.0025). Several groups [5,6,7,8] have reported measurements of  $D^0 \rightarrow K_S^0 K_S^0 K_S^0$ .

## 6 The $D^0 \rightarrow K_S^0 K_S^0$ Decay Mode

The  $D^0 \rightarrow K^0 \bar{K}^0$  decay is expected to occur primarily via two  $W$ -exchange diagrams, which are expected to cancel out in a four-quark model. In the standard six-quark model the difference between the two amplitudes is tiny, proportional to  $SU(3)$  flavour breaking effects, and we thus might expect the branching fraction for the decay to be very small ( $< 3 \times 10^{-4}$ ). However, a Standard Model based calculation [10] predicts a relatively large branching fraction due to final-state interaction effects, leading to a branching ratio of  $B(D^0 \rightarrow K^0 \bar{K}^0) = \frac{1}{2} B(D^0 \rightarrow K^+ K^-) = 0.3\%$ . A recent investigation [11] has focused on the  $s$ -channel and the  $t$ -channel one particle exchange (OPE) contributions. While the  $s$ -channel contribution, taken into account through the poorly known scalar meson  $f_0(1710)$ , gives a small contribution, the one particle  $t$ -exchange gives higher contributions, with pion exchange being the highest. In the factorization limit [12], the branching fraction is expected to be equal to zero. Non-factorizable contributions in factorization-type models have been recently studied [13] and predict a branching fraction of about  $10^{-4}$ . Several experiments [14,15,16,17] have reported measurements of  $D^0 \rightarrow$

$K_S^0 K_S^0$ .

This channel is similar to  $D^0 \rightarrow K_S^0 K_S^0 K_S^0$  in that no  $L/\sigma_L$  cut is possible, but the channel requires an additional  $D^*$  tag requirement. We select  $D^{*+}$  candidates by requiring that the reconstructed mass difference  $\Delta M = M_{D^{*+}} - M_{D^0}$  lies within 2 MeV/ $c^2$  of the nominal mass difference [18] of 145.42 MeV/ $c^2$ .

The dominant background sources for  $D^0 \rightarrow K_S^0 K_S^0$  decays are from non-resonant  $K_S^0 \pi^+ \pi^-$  and  $\pi^+ \pi^- \pi^+ \pi^-$  decays. To reduce feedthrough from  $D^0 \rightarrow K_S^0 \pi^+ \pi^-$  where the  $\pi^+ \pi^-$  invariant mass falls in  $K_S^0$  mass region or from  $D^0 \rightarrow \pi^+ \pi^- \pi^+ \pi^-$  where both  $\pi^+ \pi^-$  pairs can be misidentified as  $K_S^0$  candidates, we make the additional requirement that the  $K_S^0$  candidates reconstructed with silicon strip informations have a decay length significance ( $L/\sigma_L$ ) greater than 12. We also apply a  $|\cos \theta_{K_S^0}| < 0.8$  cut, where  $\theta_{K_S^0}$  is the angle between the  $K_S^0$  momentum in the  $D^0$  rest frame and the  $D^0$  laboratory momentum.

In Fig. 3a the  $K_S^0 K_S^0$  invariant mass distribution is shown for the events satisfying these cuts. For the signal shape we use a double Gaussian (two Gaussians with the same mean) for the  $D^0$  signal ( $79 \pm 17$  events), as suggested by Monte Carlo studies, and a first order Chebyshev polynomial for the background. The double Gaussian shape is fixed to the one obtained from Monte Carlo simulation. In Fig. 3b the  $\Delta M = D^{*+} - D^0$  mass difference distribution in the  $D^0$  mass region is plotted. A Gaussian is used to fit the signal while for the background we use the functional form

$$a(\Delta M - m_\pi)^{1/2} + b(\Delta M - m_\pi)^{3/2} \quad (3)$$

where  $m_\pi$  is the pion mass, the first term is from a non-relativistic model of phase space and the second term is the first-order relativistic correction to the non-relativistic model. Consistent yields are obtained from the two fits.

The events of the normalization mode  $D^0 \rightarrow K_S^0 \pi^+ \pi^-$  have been selected using the same reconstruction and fitting techniques as for  $D^0 \rightarrow K_S^0 K_S^0$  mode and similar selection criteria to minimize systematic uncertainties.

We measure

$$\frac{\Gamma(D^0 \rightarrow K_S^0 K_S^0)}{\Gamma(D^0 \rightarrow K_S^0 \pi^+ \pi^-)} = \frac{\Gamma(D^0 \rightarrow K^0 \bar{K}^0)}{\Gamma(D^0 \rightarrow \bar{K}^0 \pi^+ \pi^-)} = 0.0144 \pm 0.0032 \pm 0.0016. \quad (4)$$

This accounts for the unseen  $K_L^0 \pi^+ \pi^-$  and  $K_L^0 K_L^0$  decays (note that  $D^0 \rightarrow K_S^0 K_L^0$  is forbidden by CP conservation). Different systematic sources have been investigated and the value reported includes contributions from fit variations (0.0013) and  $K_S^0$  reconstruction (0.0010).



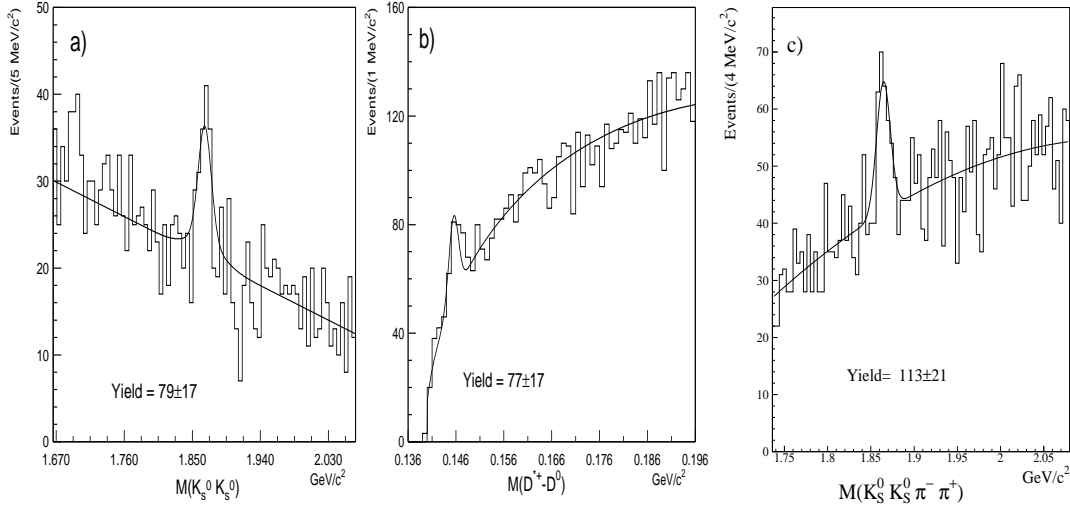


Fig. 3. Invariant mass distribution for various  $D^0$  final states: (a) Reconstructed mass of  $D^0 \rightarrow K_S^0 K_S^0$  with a  $D^{*+} - D^0$  mass difference cut. There are  $79 \pm 17$  events with a sigma of  $12.5 \text{ MeV}/c^2$ . (b) Reconstructed mass difference of  $D^{*+} - D^0$ ;  $D^0 \rightarrow K_S^0 K_S^0$ . There are  $77 \pm 17$  events in the mass difference plot demonstrating consistency with (a). (c) Reconstructed mass of  $D^0 \rightarrow K_S^0 K_S^0 \pi^+ \pi^-$ . There are  $113 \pm 21$  events.

## 7 The $D^0 \rightarrow K_S^0 K_S^0 \pi^+ \pi^-$ Decay Mode

This channel is Cabibbo-suppressed and was first observed by the ARGUS Collaboration [19]. It has a larger background than the  $D^0 \rightarrow K_S^0 K_S^0 K^+ \pi^-$  channel due to more phase space and two pions. In addition one must eliminate  $\pi^+ \pi^-$  combinations which are consistent with the  $K_S^0$  mass. To increase the signal to noise, a  $L/\sigma > 6$  cut is applied. In Fig. 3c we present the  $K_S^0 K_S^0 \pi^+ \pi^-$  invariant mass. The figure is fit with a Gaussian for the  $D^0$  signal plus a  $2^{nd}$  order polynomial.

As the resonant structure for this channel is not known, we use a non-resonant Monte Carlo simulation to compute the branching fraction.

A  $D^0 \rightarrow K^{*(892)-} K^{*(892)+}$  simulation is used as a measure of the systematic variation (the difference in efficiency is 7%). Again, we calculate the branching ratio of this mode with respect to the  $D^0 \rightarrow \bar{K}^0 \pi^+ \pi^-$  mode.

$$\frac{\Gamma(D^0 \rightarrow K_S^0 K_S^0 \pi^+ \pi^-)}{\Gamma(D^0 \rightarrow \bar{K}^0 \pi^+ \pi^-)} = 0.0208 \pm 0.0035 \pm 0.0021 \quad (5)$$

We have included systematic uncertainty contributions from split samples (0), fit variations (0.0013), possible resonant decay (0.0005), Monte Carlo statistics (0.0002), absolute tracking efficiency (0.0001), and the variation between  $K_S^0$  reconstruction categories (0.0015).

Table 1

 $D^0 \rightarrow K_S^0 K_S^0 X$  Branching Fractions

Decay Mode	This Experiment	PDG 2004 [18]
$\frac{\Gamma(D^0 \rightarrow K_S^0 K_S^0 K^\pm \pi^\mp)}{\Gamma(D^0 \rightarrow \bar{K}^0 \pi^+ \pi^-)}$	$0.0106 \pm 0.0019 \pm 0.0010$	-
$\frac{\Gamma(D^0 \rightarrow K_S^0 K_S^0 K_S^0)}{\Gamma(D^0 \rightarrow \bar{K}^0 \pi^+ \pi^-)}$	$0.0179 \pm 0.0027 \pm 0.0026$	$0.0154 \pm 0.0025$
$\frac{\Gamma(D^0 \rightarrow K^0 \bar{K}^0)}{\Gamma(D^0 \rightarrow \bar{K}^0 \pi^+ \pi^-)}$	$0.0144 \pm 0.0032 \pm 0.0016$	$0.0119 \pm 0.0033$
$\frac{\Gamma(D^0 \rightarrow K_S^0 K_S^0 \pi^+ \pi^-)}{\Gamma(D^0 \rightarrow \bar{K}^0 \pi^+ \pi^-)}$	$0.0208 \pm 0.0035 \pm 0.0021$	$0.031 \pm 0.010 \pm 0.008$

## 8 Conclusions

We summarize our branching ratios and compare them in Table I to the Particle Data Group world averages where available [18].

We have investigated and measured the branching ratios of several decay modes of the charm meson  $D^0$  into final states containing at least two  $K_S^0$  relative to  $D^0 \rightarrow \bar{K}^0 \pi^+ \pi^-$  mode. We have evidence for two new Cabibbo favored  $D^0$  decay modes, namely  $D^0 \rightarrow K_S^0 K_S^0 K^+ \pi^-$  and  $D^0 \rightarrow K_S^0 K_S^0 K^- \pi^+$  and we have reported new measurements for  $D^0 \rightarrow K_S^0 K_S^0 K_S^0$ ,  $D^0 \rightarrow K_S^0 K_S^0$ , and  $D^0 \rightarrow K_S^0 K_S^0 \pi^+ \pi^-$ .

## 9 Acknowledgments

We wish to acknowledge the assistance of the staffs of Fermi National Accelerator Laboratory, the INFN of Italy, and the physics departments of the collaborating institutions. This research was supported in part by the U. S. National Science Foundation, the U. S. Department of Energy, the Italian Istituto Nazionale di Fisica Nucleare and Ministero della Istruzione Università e Ricerca, the Brazilian Conselho Nacional de Desenvolvimento Científico e Tecnológico, CONACyT-México, and the Korea Research Foundation of the Korean Ministry of Education.

## References

- [1] P. L. Frabetti *et al.*, E687 Collaboration, Nucl. Instrum. Meth. **A320** (1992) 519.
- [2] J. M. Link *et al.*, FOCUS Collaboration, Nucl. Instrum. Meth. **A516** (2004) 364.

- [3] J. M. Link *et al.*, FOCUS Collaboration, Nucl. Instrum. Meth. **A484** (2002) 270.
- [4] J. M. Link *et al.*, FOCUS Collaboration, Nucl. Instrum. Meth. **A484** (2002) 174.
- [5] H. Albrecht *et al.*, ARGUS Collaboration, Z. Phys. **C46** (1990) 9.
- [6] R. Ammar *et al.*, CLEO Collaboration, Phys. Rev. **D44** (1991) 1941.
- [7] P. L. Frabetti *et al.*, E687 Collaboration, Phys. Lett. **B340** (1994) 254.
- [8] D. M. Asner *et al.*, CLEO Collaboration, Phys. Rev. **D54** (1996) 4211.
- [9] A. Czarnecki *et al.*, Z. Phys. **C54** (1992) 411.
- [10] X. Y. Pham, Phys. Lett. **B193** (1987) 331.
- [11] Y. S. Dai *et al.*, Phys. Rev. **D60** (1999) 014014.
- [12] M. Bauer *et al.*, Z. Phys. **C34** (1987) 103.
- [13] J. O. Eeg *et al.*, Phys. Rev. **D64** (2001) 034010.
- [14] D. M. Asner *et al.*, CLEO Collaboration, Phys. Rev. **D54** (1996) 4211.
- [15] P. L. Frabetti *et al.*, E687 Collaboration, Phys. Lett. **B340** (1994) 254.
- [16] J. Alexander *et al.*, CLEO Collaboration, Phys. Rev. Lett. **65** (1990) 1184.
- [17] J. P. Cumalat *et al.*, E400 Collaboration, Phys. Lett. **B210** (1988) 253.
- [18] S. Eidelman *et al.*, Particle Data Group, Phys. Lett. **B592** (2004) 1.
- [19] H. Albrecht *et al.*, ARGUS Collaboration, Z. Phys. **C64** (1994) 375.